SPACE TELESCOPE SCIENCE INSTITUTE
Operated for NASA by AURA

Instrument Science Report WFC3 2005-06

WFC3 Thermal Vacuum Testing: IR Grism Focus and Tilt Anomalies

H. Bushouse and G. F. Hartig
February 9, 2005

ABSTRACT

The WFC3 thermal-vacuum testing performed in the Fall of 2004 has revealed anomalies concerning the two grisms installed in the IR channel of the instrument. First, the grisms do not produce in-focus images, the cause of which has been traced to a 90 degree rotation error in the way the grisms were mounted in the filter wheel. Second, both grisms show a residual tilt of their dispersion axes relative to the detector axes of ~8.3 degrees, which is far larger than what would be expected from random uncertainties in their mounting.

1. Introduction

The Wide Field Camera 3 (WFC3) InfraRed (IR) channel employs two grisms for slitless spectroscopy. The G102 grism covers an approximate wavelength range of 0.8-1.1 microns and the G141 covers the range 1.1-1.7 microns. A set of tests were performed for each of these grisms during the WFC3 thermal-vacuum testing that took place in September-October 2004. The original goal of these tests was to measure the dispersion and other spectral trace properties of the grisms. This was the first time that exposures were obtained with the IR grisms after they were integrated with the instrument. These dispersion measurements comprised test procedures IR16S01 for the G102 grism and IR16S02 for the G141 (see ISR WFC3-2004-03).

The tests were successful in obtaining suitable data from which the dispersion properties of the grisms could be measured (reported separately in ISR WFC3-2005-07). Inspection of the data, however, immediately revealed two anomalies associated with the IR grisms. First, neither grism produced in-focus images at the plane of the WFC3 IR detector. The

cross-dispersion FWHM of spectra produced from point sources was significantly larger than that obtained in direct images. Second, it was noticed that the spectra produced by both grisms have a tilt of ~8.3 degrees relative to the nearest detector axis. The goal was to have the grisms aligned so that the spectra were parallel to one detector axis to within 1 degree.

Based on these initial results, a set of additional tests were devised to further characterize the anomalies. The following sections provide the details of those tests and their results. All test exposures were obtained under vacuum conditions, with the WFC3 detectors and optical bench at flight-like temperatures. The LD1060 and LD1310 laser diodes in the CASTLE optical stimulus system were used to present point sources to the G102 and G141 grisms, respectively. The laser diodes have nominal central wavelengths of 1062 and 1311 nm. Normally the laser diodes provide an extremely narrow-band source, on the order of 1-3nm in bandwidth. However, for the majority of the test exposures used in this investigation, it was necessary to run the diodes at a very low current level, in order to avoid saturating the detected source. At low current levels the diode emission covers a much larger range in wavelength, as can be seen from the extent of the dispersed images shown in subsequent sections. This does not affect the results of the tests in any way.

2. Spectrum Tilt

The dispersion measurement test procedures, IR16S01 and IR16S02, each included a grism-dispersed image of a white-light source, which shows the spatial location of the spectrum produced by each grism. Examples of these images are shown in Figure 1. The direction of dispersion (direction of increasing wavelength) in these images is from left to right, approximately parallel with the horizontal or x-axis of the images. It is obvious from these images, however, that the dispersion is not precisely parallel to the x-axis. Fits to the spectral traces indicate that the spectrum in the G102 image is tilted away from the x-axis at an angle of 8.25 +/- 0.1 degrees and at an angle of 8.5 +/- 0.1 degrees in the G141 image.

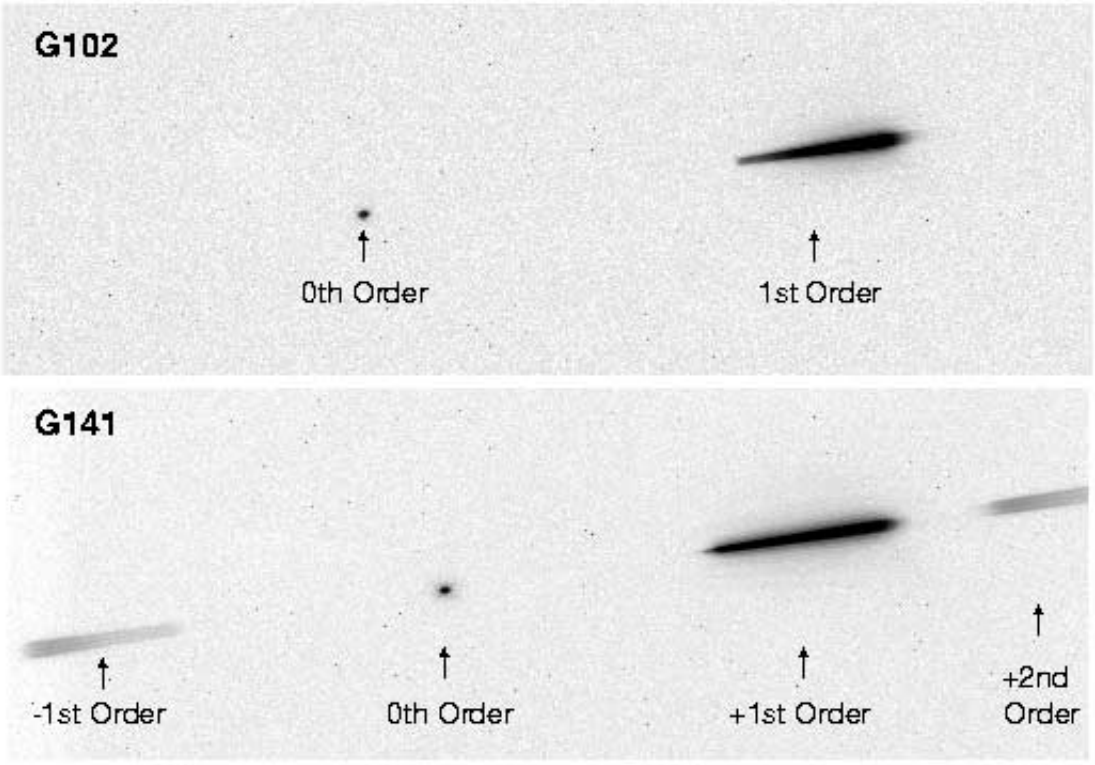

Figure 1: Dispersed images of a white-light point source through the G102 (top) and G141 (bottom) grisms. The dispersion axis is tilted by ~8.3 degrees relative to the x (horizontal) axis of the images.

3. Focus Investigation

Figure 2 shows close-up views of the first-order spectra produced by a white-light point source through the G102 and G141 grisms at the nominal WFC3 and optical stimulus focus settings. Figure 3 shows cross-dispersion plots of these spectral profiles, as well as the equivalent profile for the same undispersed source imaged through the F105W filter. The spatial profile widths of the spectra are obviously much larger than that of the undispersed source (8-10 pixels FWHM versus ~1.4 pixels). In the G102 spectral image the rather obvious triple-peaked profile is due to the severely out of focus “doughnut-like” source being dispersed along the x-axis of the image.

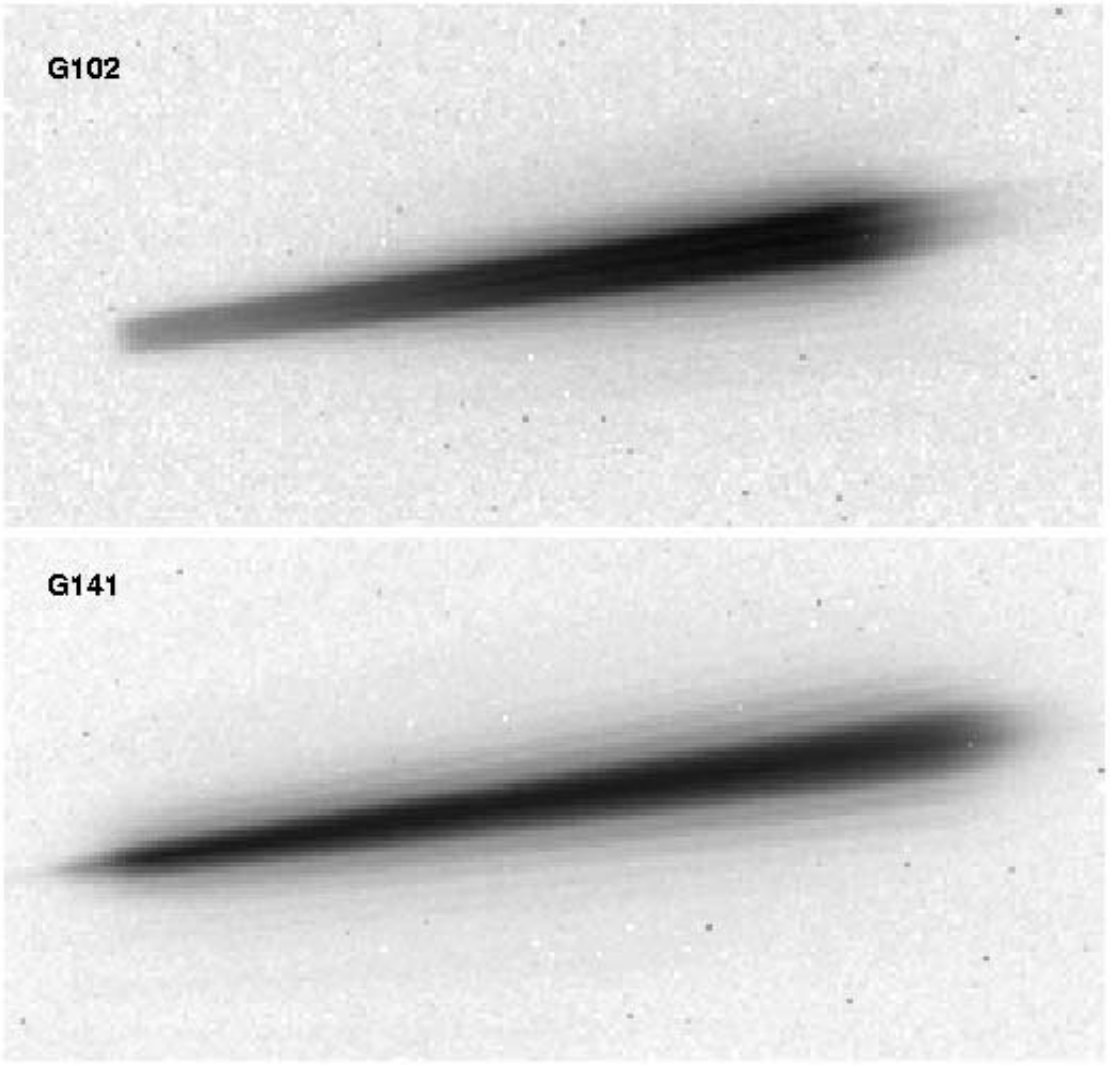

Figure 2: Close-up views of the first-order white-light spectra produced by the G102 (top) and G141 (bottom) grisms at the nominal WFC3 and stimulus focus settings.

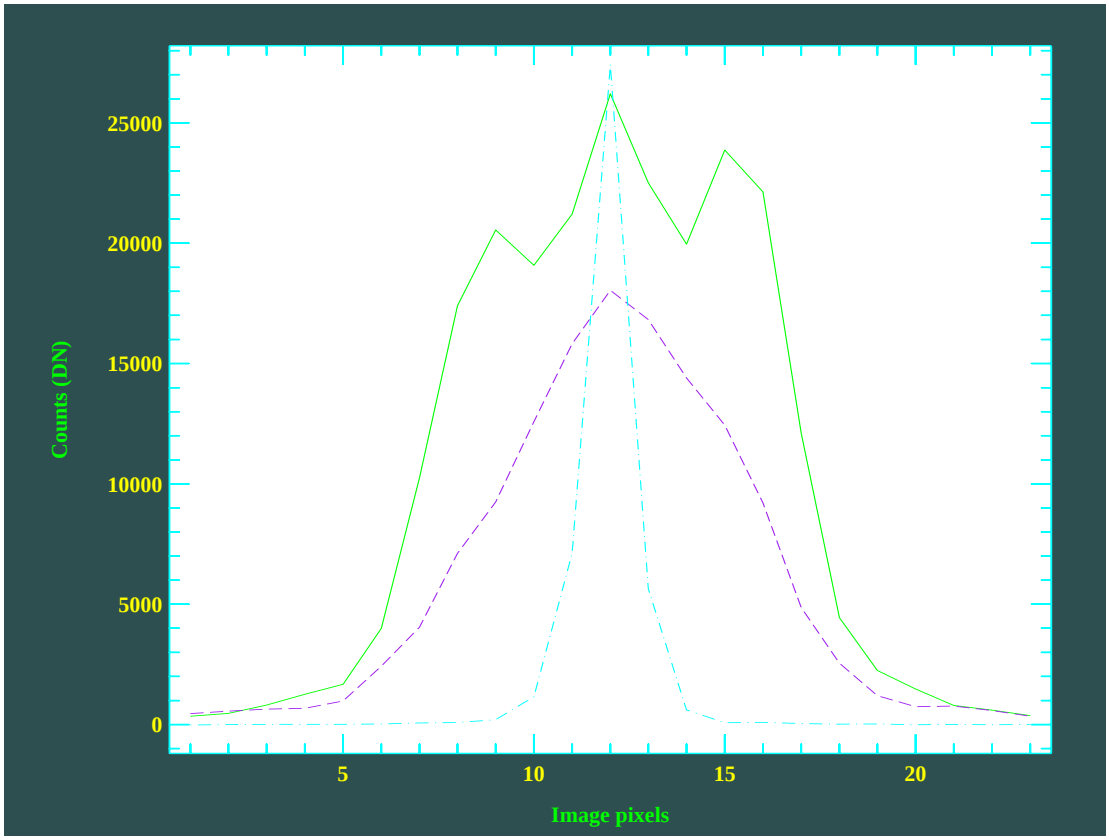

Figure 3: Crosscut plots of dispersed sources through the G102 (solid green line) and G141 (dashed magenta line) grisms, and the same source undispersed through the F105W filter (dot-dash blue line). All images obtained at nominal WFC3 and stimulus focus.

3.1. Focus at Field Center

After the initial discovery of the out of focus grism images, a decision was made to further investigate and characterize the nature of the problem with additional tests. Two sets of new tests were executed for each grism. First, a focus sweep was performed for a point source located near the center of the IR field of view in order to determine if the grisms could produce a focused image at any setting. These tests were conducted using two new SMS's, IR16S03 and IR16S04, for the G102 and G141 grisms, respectively. For these tests the internal WFC3 IR focus and corrector settings were left at their nominal positions while the focus of the external optical stimulus (CASTLE) was varied from -35mm to +10mm relative to its nominal position. The LD1060 and LD1310 CASTLE laser diodes were used as the sources for the G102 and G141 images, respectively.

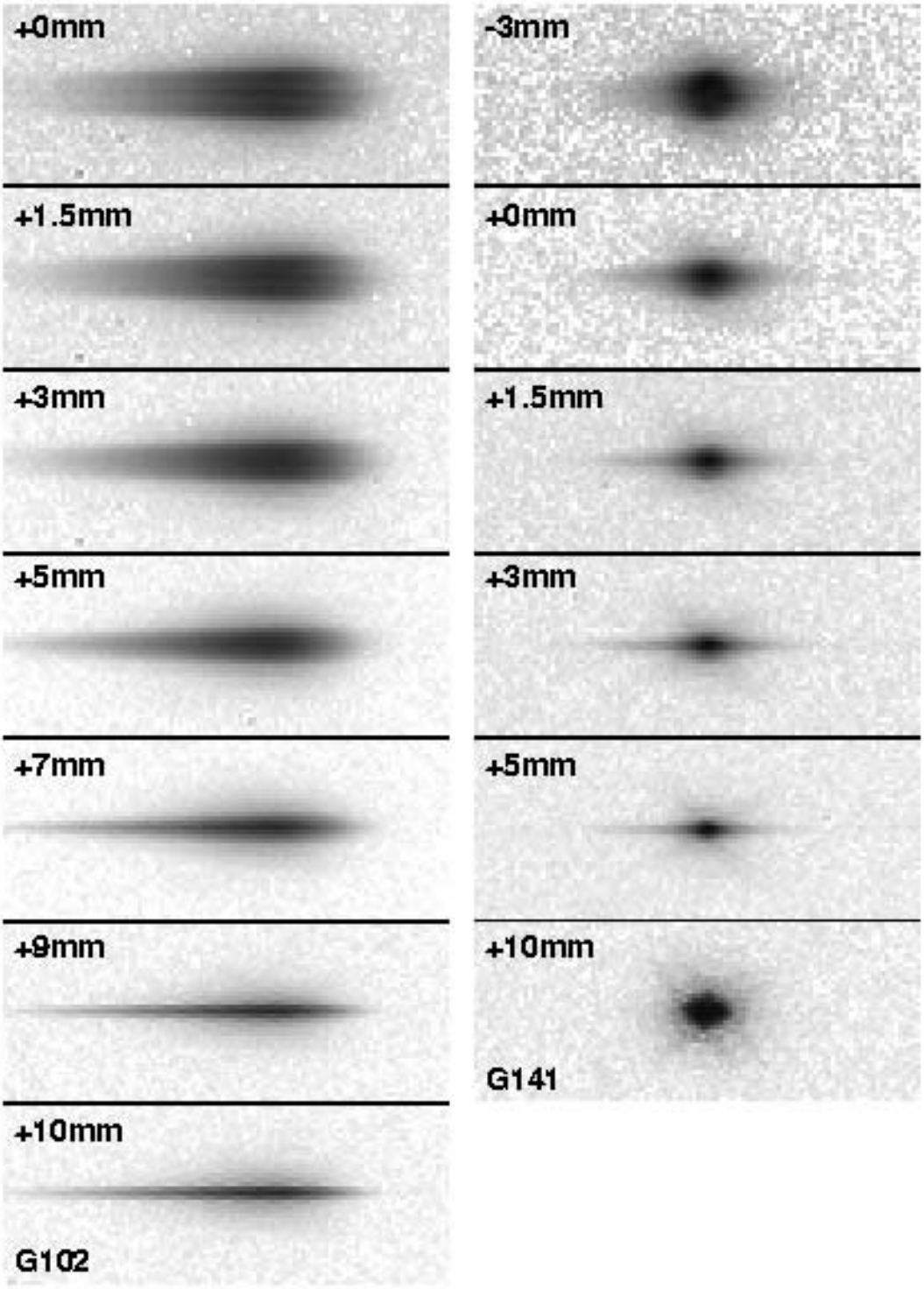

Figure 4: A subset of the center-of-field focus sweep images for the grisms. Both grisms come into focus, at least at one wavelength, in the +5 to +10mm range of CASTLE focus.

Figure 4 shows a subset of the images obtained from the focus sweep tests. Table 1 lists the cross-dispersion FWHM measurements from the G102 focus sweep images and Table 2 contains the results from the G141. These data are also plotted in Figure 5. These figures demonstrate that it is possible to bring both grisms into focus, at least for the wavelength of the source that was used, somewhere near CASTLE focus offset positions of +5 to +10mm. The nominal conversion factor to translate from CASTLE focus mechanism offsets to an equivalent offset at the IR detector plane is ~0.25 (G. Hartig, private communication). Thus the CASTLE offset of +10mm for the G102 grism corresponds to about 2.5mm at the detector.

Figure 5 also shows that the different spectral orders come into focus at different settings. For the G102, the zero-order spot comes into best focus at about the -5mm CASTLE setting, while the first-order spectrum comes into best focus at about +10mm. Similarly, the G141 zero-order spot reaches best focus near a CASTLE setting of -2mm, while the first-order spectrum is in focus near +5mm (note that the one image obtained at +10mm for the G141 is moderately saturated and therefore the FWHM measurement is uncertain). We were also able to obtain measurements for the negative first-order light in the G141 test images. This order comes into best focus at a CASTLE setting of about -13mm.

3.2. Focus vs. Field Position

Upon discovering that both grisms could be brought to a focus at the center of the field of view, an additional test was executed to determine whether the best focus varied with field position. The SMS's IR16S05 and IR16S06 were used to take a short focus sweep of a source at 9 different field points, evenly distributed across the field of view in a 3x3 pattern, for each of the grisms. A 3-position focus sweep was executed at each field point, consisting of CASTLE focus offsets of 0, +5, and +10mm.

The FWHM of the resulting spectra are shown in Figure 6 for the G102 and Figure 7 for the G141. Two things are evident from these results. First, neither grism produces focused images at the nominal focus setting (CASTLE offset = 0mm) anywhere within the IR field of view. Second, the position of best focus does depend somewhat on field position. For example, from Figure 6 we can see that the CASTLE offset that gives the best focus varies diagonally across the detector. Near the lower left-hand corner of the field (corresponding to image pixel coordinates 0x0) the difference in focus between the +5mm and +10mm settings is minimized, while in the upper right-hand corner (image pixel coordinates 1024x1024) it is maximized. Similarly, in Figure 7 we see that the difference in focus between the 0mm and +5mm CASTLE offsets is minimized in the lower left-hand corner of the field, while it is maximized at the upper right. So for both grisms, we see that the position of best focus shifts from lower offsets in the bottom left to larger offsets in the top right.

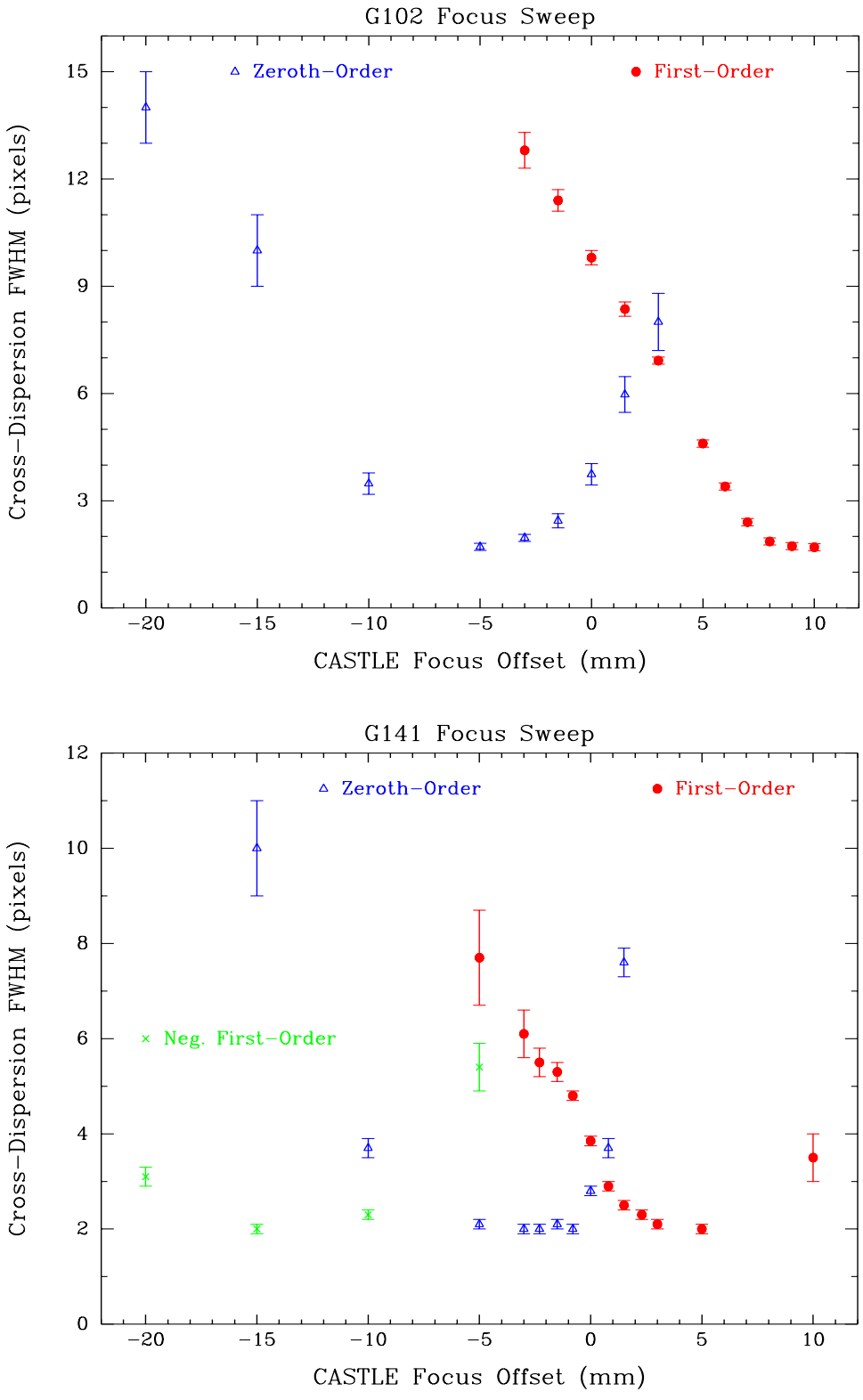

Figure 5: Cross-dispersion FWHM measurements from the focus sweep images.

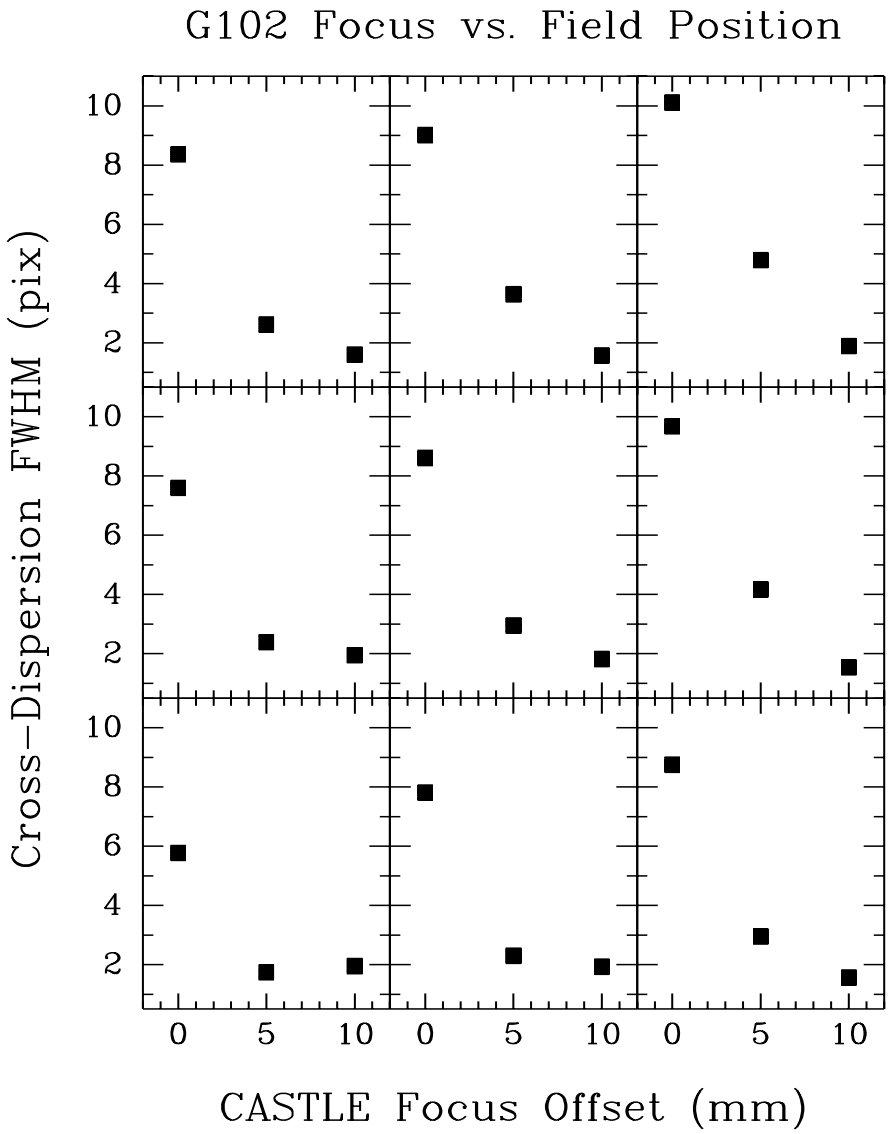

Figure 6: G102 focus versus field position. The 9 field points were evenly distributed in a 3x3 grid across the field of view.

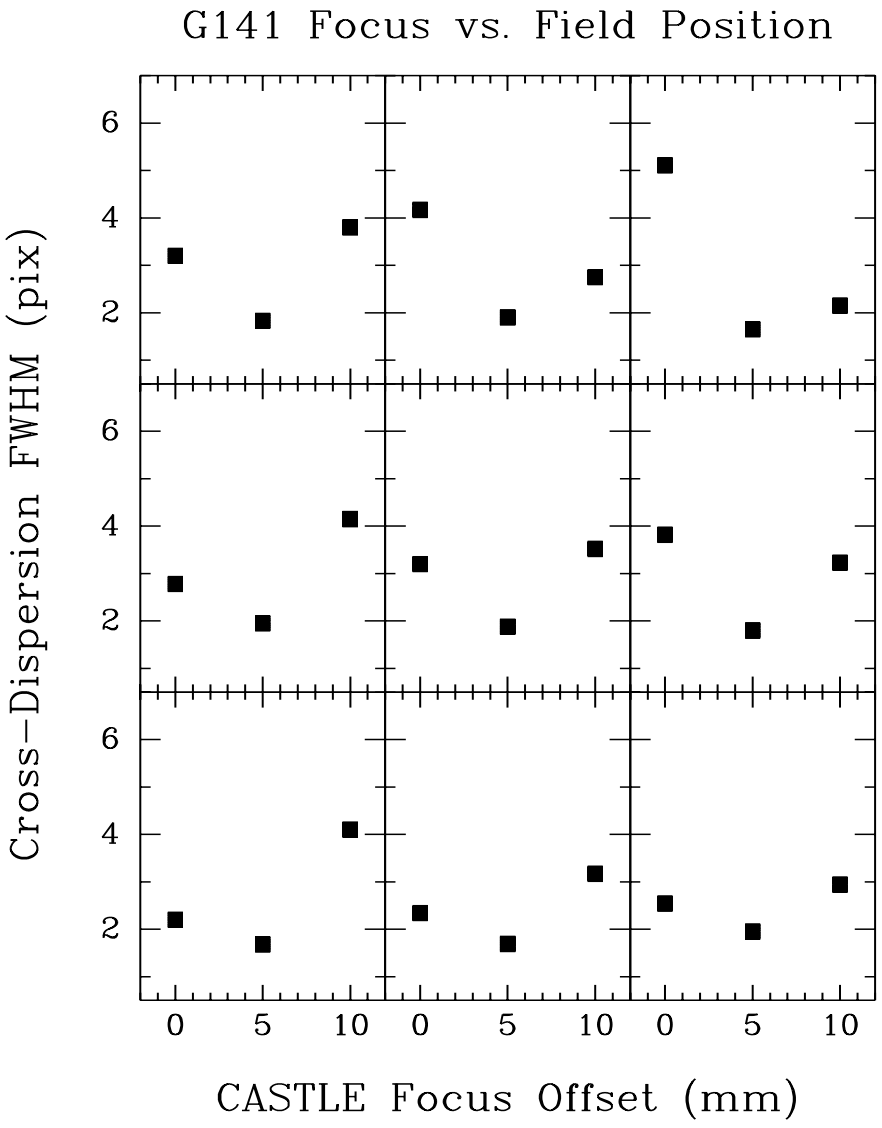

Figure 7: G141 focus versus field position. The 9 field points were evenly distributed in a 3x3 grid across the field of view.

3.3. Internal Focus Correction Test

A final test was performed in which the WFC3 IR channel internal focus and corrector mechanisms were adjusted to determine whether the grism focus offsets were within the range of the internal mechanisms. A set of 23 exposures was obtained manually for the G102 grism, leaving the CASTLE at its nominal focus setting, while iteratively applying adjustments to the IR focus, and inner and outer corrector mechanisms, until a best focus image was obtained. The set of images in this test corresponds to WFC3 test exposure numbers (TVNUM) 18301-18323, obtained on October 8-9, 2004 (day of year 282). Table 3 lists the IR focus, outer corrector, and inner corrector mechanism settings for nominal focus (i.e. those used for the direct filters) and those found through this test to bring the G102 grism into focus. Figure 8 shows a comparison of the cross-dispersion spectral profiles for the nominal and best internal focus settings. At the nominal settings the FWHM of the spectral profile is ~8.5 IR detector pixels, while at the best internal focus settings a FWHM of only 1.7 pixels was achieved.

4. Conclusions

At this time the cause of the residual spectral tilt of ~8.3 degress is not known. The fact that the tilt is nearly identical (to within the accuracy of the measurements) for the two grisms suggests that the cause is unlikely to be any type of random error in either the construction of the grisms or their insertion and alignment within the WFC3 IR Filter Select Mechanism (FSM). Analysis of a spare grism and investigation of the design, construction, and mounting specifications of the grisms are currently underway.

The defocus issue has been traced to an error in the specifications used to mount the grisms in the FSM. The specifications have been shown to have a rotation error of 90 degrees in the coordinate system used to indicate the orientation (“clocking”) of the grisms in the FSM. Optical modelling has successfully demonstrated that such a 90 degree rotation, coupled with the 24 degree tilt of the IR detector, exactly reproduces the character of the defocus that has been seen, including the relative focus offsets of the different spectral orders.

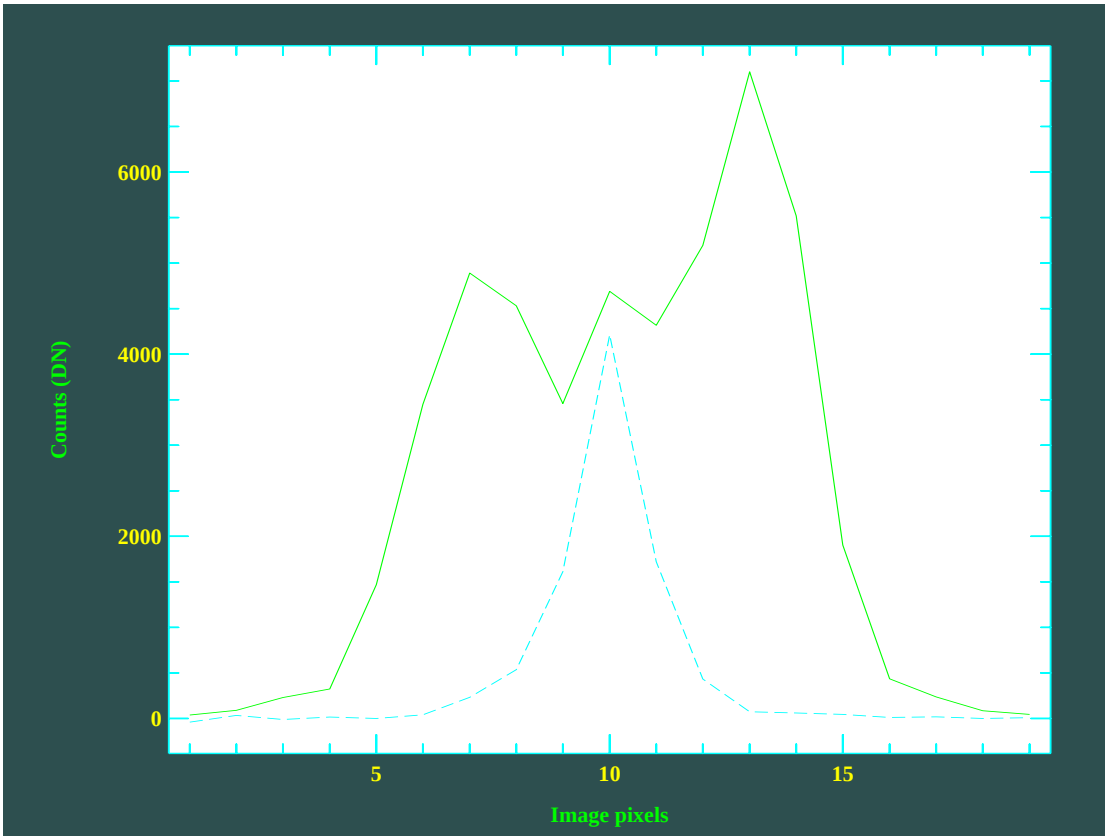

Figure 8: Crosscut plots of the G102 spectral profile at nominal focus settings (solid green line) and using the best internal IR focus corrector settings (dashed blue line).

Table 1. G102 Focus Sweep FWHM Measurements

Zeroth Order			Positive First Order		
Focus Offset (mm)	**FWHM** (pixels)	σ (pixels)	**Focus Offset** (mm)	**FWHM** (pixels)	σ (pixels)
-20.0	14.0	1.0	-3.0	12.8	0.8
-15.0	10.0	1.0	-1.5	11.4	0.5
-10.0	3.5	0.3	0.0	9.8	0.3
-5.0	1.7	0.1	+1.5	8.4	0.2
-3.0	2.0	0.1	+3.0	6.9	0.2
-1.5	2.4	0.2	+5.0	4.6	0.1
0.0	3.7	0.3	+6.0	3.4	0.1
+1.5	6.0	0.5	+7.0	2.4	0.1
+3.0	8.0	0.8	+8.0	1.9	0.1
			+9.0	1.7	0.1
			+10.0	1.7	0.1

Table 2. G141 Focus Sweep FWHM Measurements

Negative First Order			Zeroth Order			Positive First Order		
Focus Offset (mm)	**FWHM** (pixels)	σ (pixels)	**Focus Offset** (mm)	**FWHM** (pixels)	σ (pixels)	**Focus Offset** (mm)	**FWHM** (pixels)	σ (pixels)
-35.0	19.0	2.0	-20.0	15.0	2.0	-10.0	17.0	2.0
-20.0	3.1	0.2	-15.0	10.0	1.0	-5.0	7.7	1.0
-15.0	2.0	0.1	-10.0	3.7	0.2	-3.0	6.1	0.5
-10.0	2.3	0.1	-5.0	2.1	0.1	-2.25	5.5	0.3
-5.0	5.4	0.5	-3.0	2.0	0.1	-1.5	5.3	0.2
			-2.25	2.0	0.1	-0.75	4.8	0.1
			-1.5	2.1	0.1	0.0	3.9	0.1
			-0.75	2.0	0.1	+0.75	2.9	0.1
			0.0	2.8	0.1	+1.5	2.5	0.1
			+0.75	3.7	0.2	+2.25	2.3	0.1
			+1.5	7.6	0.3	+3.0	2.1	0.1
						+5.0	2.0	0.1
						+10.0	3.5	0.5

Table 3. Internal IR Corrector Settings

	Nominal	**Best Focus**
IRFOCPOS	2411	2996
IROUTRES	42407	35426
IRINNRES	53171	45132
FWHM (pix)	~8.5	1.7